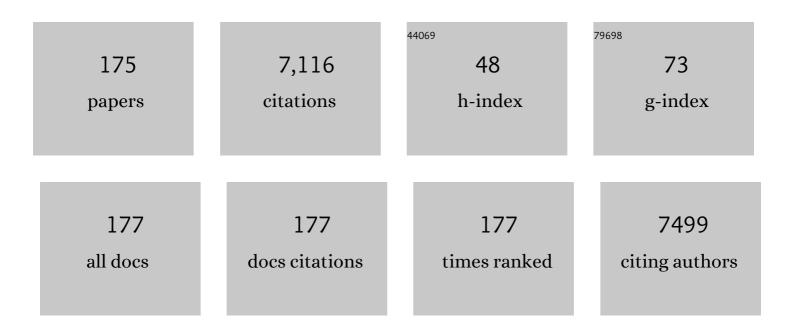
List of Publications by Year in descending order

Source: https://exaly.com/author-pdf/843079/publications.pdf Version: 2024-02-01



#	Article	IF	CITATIONS
1	Supported catalysts based on layered double hydroxides for catalytic oxidation and hydrogenation: general functionality and promising application prospects. Chemical Society Reviews, 2015, 44, 5291-5319.	38.1	306
2	Low-temperature hydrothermal synthesis of WO3 nanorods and their sensing properties for NO2. Journal of Materials Chemistry, 2012, 22, 12643.	6.7	203
3	Ultra-sensitive ethanol gas sensors based on nanosheet-assembled hierarchical ZnO-In2O3 heterostructures. Journal of Hazardous Materials, 2020, 391, 122191.	12.4	162
4	Synthesis mechanism and gas-sensing application of nanosheet-assembled tungsten oxide microspheres. Journal of Materials Chemistry A, 2014, 2, 7927-7934.	10.3	153
5	Ultrathin and Vacancy-Rich CoAl-Layered Double Hydroxide/Graphite Oxide Catalysts: Promotional Effect of Cobalt Vacancies and Oxygen Vacancies in Alcohol Oxidation. ACS Catalysis, 2018, 8, 3104-3115.	11.2	149
6	Electrocatalytic Cobalt Nanoparticles Interacting with Nitrogen-Doped Carbon Nanotube in Situ Generated from a Metal–Organic Framework for the Oxygen Reduction Reaction. ACS Applied Materials & Interfaces, 2017, 9, 2541-2549.	8.0	137
7	Synthesis of MoO3/reduced graphene oxide hybrids and mechanism of enhancing H2S sensing performances. Sensors and Actuators B: Chemical, 2015, 216, 113-120.	7.8	135
8	Quantum-sized ZnO nanoparticles: Synthesis, characterization and sensing properties for NO2. Journal of Materials Chemistry, 2011, 21, 12288.	6.7	131
9	Pd nanoparticles on hydrotalcite as an efficient catalyst for partial hydrogenation of acetylene: Effect of support acidic and basic properties. Journal of Catalysis, 2015, 331, 118-127.	6.2	126
10	Mechanism enhancing gas sensing and first-principle calculations of Al-doped ZnO nanostructures. Journal of Materials Chemistry A, 2013, 1, 11335.	10.3	125
11	Recent Progress on Rational Design of Bimetallic Pd Based Catalysts and Their Advanced Catalysis. ACS Catalysis, 2020, 10, 13560-13583.	11.2	124
12	Interfacial Structure-Determined Reaction Pathway and Selectivity for 5-(Hydroxymethyl)furfural Hydrogenation over Cu-Based Catalysts. ACS Catalysis, 2020, 10, 1353-1365.	11.2	118
13	Facile synthesis of mesoporous hierarchical Co ₃ O ₄ –TiO ₂ p–n heterojunctions with greatly enhanced gas sensing performance. Journal of Materials Chemistry A, 2017, 5, 10387-10397.	10.3	116
14	Polythiophene-WO3 hybrid architectures for low-temperature H2S detection. Sensors and Actuators B: Chemical, 2014, 197, 142-148.	7.8	111
15	Layered double hydroxide-derived Ni-Cu nanoalloy catalysts for semi-hydrogenation of alkynes: Improvement of selectivity and anti-coking ability via alloying of Ni and Cu. Journal of Catalysis, 2018, 359, 251-260.	6.2	111
16	Facile Synthesis and Acetone Sensing Performance of Hierarchical SnO ₂ Hollow Microspheres with Controllable Size and Shell Thickness. Industrial & Engineering Chemistry Research, 2016, 55, 3588-3595.	3.7	103
17	On the construction of hollow nanofibers of ZnO-SnO2 heterojunctions to enhance the NO2 sensing properties. Sensors and Actuators B: Chemical, 2018, 266, 692-702.	7.8	96
18	Layered and intercalated hydrotalcite-like materials as thermal stabilizers in PVC resin. Journal of Physics and Chemistry of Solids, 2006, 67, 998-1001.	4.0	93

DIANQING LI

#	Article	IF	CITATIONS
19	Partial hydrogenation of acetylene using highly stable dispersed bimetallic Pd–Ga/MgO–Al2O3 catalyst. Journal of Catalysis, 2014, 309, 166-173.	6.2	92
20	Au–Pd nanoalloys supported on Mg–Al mixed metal oxides as a multifunctional catalyst for solvent-free oxidation of benzyl alcohol. Dalton Transactions, 2013, 42, 14498.	3.3	91
21	Gas sensing properties of Cd-doped ZnO nanofibers synthesized by the electrospinning method. Journal of Materials Chemistry A, 2014, 2, 16697-16706.	10.3	86
22	Sensing performance and mechanism of Fe-doped ZnO microflowers. Sensors and Actuators B: Chemical, 2014, 195, 657-666.	7.8	85
23	Surface functionalization of Co3O4 hollow spheres with ZnO nanoparticles for modulating sensing properties of formaldehyde. Sensors and Actuators B: Chemical, 2017, 245, 359-368.	7.8	82
24	Highly efficient PdAg catalyst using a reducible Mg-Ti mixed oxide for selective hydrogenation of acetylene: Role of acidic and basic sites. Journal of Catalysis, 2017, 348, 135-145.	6.2	81
25	Palladium phosphide nanoparticles as highly selective catalysts for the selective hydrogenation of acetylene. Journal of Catalysis, 2018, 364, 406-414.	6.2	80
26	Surface decoration of WO3 architectures with Fe2O3 nanoparticles for visible-light-driven photocatalysis. CrystEngComm, 2014, 16, 3289.	2.6	78
27	Preparation of conducting films based on α-MoO 3 /PANI hybrids and their sensing properties to triethylamine at room temperature. Sensors and Actuators B: Chemical, 2017, 239, 131-138.	7.8	78
28	Size-controlled hydrothermal synthesis and high electrocatalytic performance of CoS2 nanocatalysts as non-precious metal cathode materials for fuel cells. Journal of Materials Chemistry A, 2013, 1, 5741.	10.3	77
29	Catalytic performance of Pd-promoted Cu hydrotalcite-derived catalysts in partial hydrogenation of acetylene: effect of Pd–Cu alloy formation. Catalysis Science and Technology, 2016, 6, 3027-3037.	4.1	76
30	Fabrication of a PdAg mesocrystal catalyst for the partial hydrogenation of acetylene. Journal of Catalysis, 2015, 330, 61-70.	6.2	68
31	SnO ₂ @Co ₃ O ₄ p–n heterostructures fabricated by electrospinning and mechanism analysis enhanced acetone sensing. RSC Advances, 2014, 4, 62862-62868.	3.6	65
32	Fabrication of supported PdAu nanoflower catalyst for partial hydrogenation of acetylene. Journal of Catalysis, 2014, 317, 263-271.	6.2	65
33	Identification of the Au/ZnO interface as the specific active site for the selective oxidation of the secondary alcohol group in glycerol. Journal of Catalysis, 2019, 369, 222-232.	6.2	65
34	The effect of oxygen vacancies in ZnO at an Au/ZnO interface on its catalytic selective oxidation of glycerol. Journal of Catalysis, 2019, 377, 271-282.	6.2	64
35	Fabrication and Bifunctional Electrocatalytic Performance of Ternary CoNiMn Layered Double Hydroxides/Polypyrrole/Reduced Graphene Oxide Composite for Oxygen Reduction and Evolution Reactions. Electrochimica Acta, 2017, 245, 59-68.	5.2	63
36	Pd/MgAl-LDH nanocatalyst with vacancy-rich sandwich structure: Insight into interfacial effect for selective hydrogenation. Journal of Catalysis, 2019, 370, 107-117.	6.2	62

DIANQING LI

#	Article	IF	CITATIONS
37	Room temperature triethylamine sensing properties of polyaniline–WO ₃ nanocomposites with p–n heterojunctions. RSC Advances, 2016, 6, 2687-2694.	3.6	61
38	Facile preparation of SnO2/NiO composites and enhancement of sensing performance to NO2. Sensors and Actuators B: Chemical, 2017, 249, 22-29.	7.8	59
39	Hydrotalcite-like MgMnTi non-precious-metal catalyst for solvent-free selective oxidation of alcohols. Journal of Catalysis, 2015, 331, 154-161.	6.2	58
40	Evolution of palladium sulfide phases during thermal treatments and consequences for acetylene hydrogenation. Journal of Catalysis, 2018, 364, 204-215.	6.2	58
41	Synthesis and selective IR absorption properties of iminodiacetic-acid intercalated MgAl-layered double hydroxide. Journal of Solid State Chemistry, 2010, 183, 1114-1119.	2.9	56
42	Highly selective and stable PdNi catalyst derived from layered double hydroxides for partial hydrogenation of acetylene. Applied Catalysis A: General, 2015, 500, 3-11.	4.3	55
43	Insight into the Effect of Dual Active Cu ⁰ /Cu ⁺ Sites in a Cu/ZnO-Al ₂ O ₃ Catalyst on 5-Hydroxylmethylfurfural Hydrodeoxygenation. ACS Sustainable Chemistry and Engineering, 2020, 8, 15288-15298.	6.7	55
44	Improved thermal and photostability of an anthraquinone dye by intercalation in a zinc–aluminum layered double hydroxides host. Dyes and Pigments, 2011, 90, 253-258.	3.7	54
45	Doping Metal Elements of WO ₃ for Enhancement of NO ₂ -Sensing Performance at Room Temperature. Industrial & Engineering Chemistry Research, 2017, 56, 2616-2623.	3.7	53
46	Vacancy enriched ultrathin TiMgAl-layered double hydroxide/graphene oxides composites as highly efficient visible-light catalysts for CO2 reduction. Applied Catalysis B: Environmental, 2020, 270, 118878.	20.2	53
47	Template-free Synthesis of Large-Pore-Size Porous Magnesium Silicate Hierarchical Nanostructures for High-Efficiency Removal of Heavy Metal Ions. ACS Sustainable Chemistry and Engineering, 2017, 5, 2774-2780.	6.7	51
48	rGO modified nanoplate-assembled ZnO/CdO junction for detection of NO2. Journal of Hazardous Materials, 2020, 394, 121832.	12.4	51
49	Adsorbate-Induced Structural Evolution of Pd Catalyst for Selective Hydrogenation of Acetylene. ACS Catalysis, 2020, 10, 15048-15059.	11.2	50
50	Preparation and structure-property relationships of supported trimetallic PdAuAg catalysts for the selective hydrogenation of acetylene. Journal of Catalysis, 2016, 344, 854-864.	6.2	49
51	Novel α-Fe2O3/BiVO4 heterojunctions for enhancing NO2 sensing properties. Sensors and Actuators B: Chemical, 2018, 268, 136-143.	7.8	49
52	Carboxyl-directed hydrothermal synthesis of WO ₃ nanostructures and their morphology-dependent gas-sensing properties. CrystEngComm, 2014, 16, 10210-10217.	2.6	47
53	Photoanode of LDH catalyst decorated semiconductor heterojunction of BiVO4/CdS to enhance PEC water splitting efficiency. International Journal of Hydrogen Energy, 2019, 44, 24642-24652.	7.1	46
54	Insight into the Role of Unsaturated Coordination O _{2c} -Ti _{5c} -O _{2c} Sites on Selective Glycerol Oxidation over AuPt/TiO ₂ Catalysts. ACS Catalysis, 2019, 9, 188-199.	11.2	45

#	Article	IF	CITATIONS
55	Support morphology effect on the selective oxidation of glycerol over AuPt/CeO2 catalysts. Journal of Catalysis, 2020, 385, 146-159.	6.2	45
56	Synthesis and Gas Sensing Performance of Dandelion-Like ZnO with Hierarchical Porous Structure. Industrial & Engineering Chemistry Research, 2014, 53, 12737-12743.	3.7	43
57	Novel Carbon Paper@Magnesium Silicate Composite Porous Films: Design, Fabrication, and Adsorption Behavior for Heavy Metal Ions in Aqueous Solution. ACS Applied Materials & Interfaces, 2018, 10, 22776-22785.	8.0	43
58	Enhancement of the Thermo- and Photostability of an Anionic Dye by Intercalation in a Zincâ^'Aluminum Layered Double Hydroxide Host. Industrial & Engineering Chemistry Research, 2008, 47, 2478-2483.	3.7	41
59	rGO decorated W doped BiVO4 novel material for sensing detection of trimethylamine. Sensors and Actuators B: Chemical, 2019, 298, 126749.	7.8	41
60	Hexamethylene tetramine-assisted hydrothermal synthesis of porous magnesium oxide for high-efficiency removal of phosphate in aqueous solution. Journal of Environmental Chemical Engineering, 2017, 5, 4649-4655.	6.7	39
61	Recent Progress on Adsorption Materials for Phosphate Removal. Recent Patents on Nanotechnology, 2019, 13, 3-16.	1.3	39
62	Novel p-n heterojunction of BiVO4/Cu2O decorated with rGO for low concentration of NO2 detection. Sensors and Actuators B: Chemical, 2020, 320, 128284.	7.8	38
63	Synthesis and UV absorption properties of 5, 5′-thiodisalicylic acid intercalated Znâ^'Al layered double hydroxides. Polymer Degradation and Stability, 2010, 95, 2082-2087.	5.8	37
64	An integrating photoanode consisting of BiVO ₄ , rGO and LDH for photoelectrochemical water splitting. Dalton Transactions, 2019, 48, 16091-16098.	3.3	37
65	Ethylene glycol-assisted fabrication and superb adsorption capacity of hierarchical porous flower-like magnesium oxide microspheres for phosphate. Inorganic Chemistry Frontiers, 2019, 6, 1952-1961.	6.0	37
66	Metal Phosphides and Sulfides in Heterogeneous Catalysis: Electronic and Geometric Effects. ACS Catalysis, 2021, 11, 9102-9127.	11.2	36
67	Highly Selective and Stable Isolated Non-Noble Metal Atom Catalysts for Selective Hydrogenation of Acetylene. ACS Catalysis, 2022, 12, 607-615.	11.2	36
68	Synthesis of a highly dispersed CuO catalyst on CoAl-HT for the epoxidation of styrene. Dalton Transactions, 2017, 46, 13463-13471.	3.3	35
69	Co - intercalation of Acid Red 337 and a UV Absorbent into Layered Double Hydroxides: Enhancement of Photostability. ACS Applied Materials & Interfaces, 2014, 6, 20603-20611.	8.0	34
70	Mechanism of enhancing the formaldehyde sensing properties of Co ₃ O ₄ via Ag modification. RSC Advances, 2015, 5, 48619-48625.	3.6	34
71	Advanced bifunctional electrocatalyst generated through cobalt phthalocyanine tetrasulfonate intercalated Ni2Fe-layered double hydroxides for a laminar flow unitized regenerative micro-cell. Journal of Power Sources, 2017, 361, 21-30.	7.8	34
72	Support morphology-dependent alloying behaviour and interfacial effects of bimetallic Ni–Cu/CeO ₂ catalysts. Chemical Science, 2019, 10, 3556-3566.	7.4	34

DIANQING LI

#	Article	IF	CITATIONS
73	Synthesis and UV Absorption Properties of Aurintricarboxylic Acid Intercalated Zn–Al Layered Double Hydroxides. Industrial & Engineering Chemistry Research, 2011, 50, 13299-13303.	3.7	33
74	Preparation of reduced graphene oxide/Co ₃ O ₄ composites and sensing performance to toluene at low temperature. RSC Advances, 2016, 6, 60109-60116.	3.6	33
75	Cu ₂ O and rGO Hybridizing for Enhancement of Low-Concentration NO ₂ Sensing at Room Temperature. Industrial & Engineering Chemistry Research, 2018, 57, 10086-10094.	3.7	33
76	Composition Tuning of Ru-Based Phosphide for Enhanced Propane Selective Dehydrogenation. ACS Catalysis, 2020, 10, 10243-10252.	11.2	33
77	Facile synthesis of multicolor organic–inorganic hybrid pigments based on layered double hydroxides. Dyes and Pigments, 2014, 104, 131-136.	3.7	31
78	Rapid synthesis of rGO–MoO ₃ hybrids and mechanism of enhancing sensing performance to H ₂ S. RSC Advances, 2015, 5, 50783-50789.	3.6	31
79	Reduced graphene oxide decorated SnO2/BiVO4 photoanode for photoelectrochemical water splitting. Journal of Alloys and Compounds, 2021, 855, 156780.	5.5	31
80	Porous ZnCl2-Activated Carbon from Shaddock Peel: Methylene Blue Adsorption Behavior. Materials, 2022, 15, 895.	2.9	31
81	rGO functionalized α-Fe2O3/Co3O4 heterojunction for NO2 detection. Sensors and Actuators B: Chemical, 2022, 354, 131194.	7.8	30
82	Controllable preparation and catalytic performance of Pd/anodic alumina oxide@Al catalyst for hydrogenation of ethylanthraquinone. Chemical Engineering Science, 2015, 135, 274-284.	3.8	29
83	Facile Fabrication of Mesoporous Hierarchical Co-Doped ZnO for Highly Sensitive Ethanol Detection. Industrial & Engineering Chemistry Research, 2019, 58, 8061-8071.	3.7	29
84	Synthesis of novel BiVO4/Cu2O heterojunctions for improving BiVO4 towards NO2 sensing properties. Journal of Colloid and Interface Science, 2020, 567, 37-44.	9.4	29
85	WO3-ZnFe2O4 heterojunction and rGO decoration synergistically improve the sensing performance of triethylamine. Sensors and Actuators B: Chemical, 2021, 347, 130619.	7.8	29
86	Fabrication of supported Pd–Ir/Al ₂ O ₃ bimetallic catalysts for 2â€ethylanthraquinone hydrogenation. AICHE Journal, 2017, 63, 3955-3965.	3.6	28
87	Low molecular weight hindered amine light stabilizers (HALS) intercalated MgAl-Layered double hydroxides: Preparation and anti-aging performance in polypropylene nanocomposites. Polymer Degradation and Stability, 2018, 154, 55-61.	5.8	28
88	Atmosphere induced amorphous and permeable carbon layer encapsulating PtGa catalyst for selective cinnamaldehyde hydrogenation. Journal of Catalysis, 2020, 389, 229-240.	6.2	28
89	Novel Strategy to Prepare Mesoporous Sn-Doped Co ₃ O ₄ Whiskers with High Sensitivity to Toluene. Industrial & Engineering Chemistry Research, 2020, 59, 4472-4482.	3.7	28
90	High Antioxidative Performance of Layered Double Hydroxides/Polypropylene Composite with Intercalation of Low-Molecular-Weight Phenolic Antioxidant. Industrial & Engineering Chemistry Research, 2014, 53, 2287-2292.	3.7	26

#	Article	IF	CITATIONS
91	Superb removal capacity of hierarchically porous magnesium oxide for phosphate and methyl orange. Environmental Science and Pollution Research, 2018, 25, 24907-24916.	5.3	26
92	Layered double hydroxides as thermal stabilizers for Poly(vinyl chloride): A review. Applied Clay Science, 2021, 211, 106198.	5.2	26
93	An α-Fe ₂ O ₃ /NiO p–n hierarchical heterojunction for the sensitive detection of triethylamine. Inorganic Chemistry Frontiers, 2020, 7, 1532-1539.	6.0	26
94	rGO decorated semiconductor heterojunction of BiVO4/NiO to enhance PEC water splitting efficiency. International Journal of Hydrogen Energy, 2022, 47, 4375-4385.	7.1	26
95	Reaction pathway investigation using in situ Fourier transform infrared technique over Pt/CuO and Pt/TiO2 for selective glycerol oxidation. Applied Catalysis B: Environmental, 2021, 291, 120061.	20.2	25
96	Mordant Yellow 3 Anions Intercalated Layered Double Hydroxides: Preparation, Thermo- and Photostability. Industrial & Engineering Chemistry Research, 2012, 51, 10542-10545.	3.7	24
97	Triadic Layered Double Hydroxide Modified Semiconductor Heterojunction for PEC Water Splitting. ACS Sustainable Chemistry and Engineering, 2020, 8, 4076-4084.	6.7	24
98	Interfacial Bifunctional Effect Promoted Non-Noble Cu/Fe <i>_y</i> MgO <i>_x</i> Catalysts for Selective Hydrogenation of Acetylene. ACS Catalysis, 2021, 11, 11117-11128.	11.2	24
99	Experimental and numerical investigation of the precipitation of barium sulfate in a rotating liquid film reactor. AICHE Journal, 2009, 55, 2024-2034.	3.6	23
100	Fabrication and Adsorption Behavior of Magnesium Silicate Hydrate Nanoparticles towards Methylene Blue. Nanomaterials, 2018, 8, 271.	4.1	23
101	Effects of zinc and manganese ions in aqueous electrolytes on structure and electrochemical performance of Na _{0.44} MnO ₂ cathode material. RSC Advances, 2016, 6, 40793-40798.	3.6	22
102	Controllable Synthesis, Structure, and Catalytic Activity of Highly Dispersed Pd Catalyst Supported on Whisker-Modified Spherical Alumina. Industrial & Engineering Chemistry Research, 2012, 51, 11083-11090.	3.7	21
103	A novel rGO-decorated ZnO/BiVO ₄ heterojunction for the enhancement of NO ₂ sensing properties. Inorganic Chemistry Frontiers, 2020, 7, 1026-1033.	6.0	21
104	Pine dendritic bismuth vanadate loaded on reduced graphene oxide for detection of low concentration triethylamine. Journal of Colloid and Interface Science, 2021, 587, 183-191.	9.4	20
105	Insights into the Role of Dual-Interfacial Sites in Cu/ZrO ₂ Catalysts in 5-HMF Hydrogenolysis with Isopropanol. ACS Applied Materials & Interfaces, 2021, 13, 22292-22303.	8.0	20
106	UV absorber co-intercalated layered double hydroxides as efficient hybrid UV-shielding materials for polypropylene. Dalton Transactions, 2019, 48, 2750-2759.	3.3	19
107	Highly efficient CuCr-MMO catalyst for a base-free styrene epoxidation with H ₂ O ₂ as the oxidant: synergistic effect between Cu and Cr. Dalton Transactions, 2019, 48, 16402-16411.	3.3	19
108	Synthesis of LaFeO3 catalytic materials and their sensing properties. Science in China Series B: Chemistry, 2009, 52, 2106-2113.	0.8	18

#	Article	IF	CITATIONS
109	Oxidation of Aliphatic Alcohols by Using Precious Metals Supported on Hydrotalcite under Solvent― and Baseâ€Free Conditions. ChemSusChem, 2015, 8, 3314-3322.	6.8	18
110	An integration system derived from LDHs for CO2 direct capture and photocatalytic coupling reaction. Chem Catalysis, 2022, 2, 531-549.	6.1	18
111	Heterostructures of polyaniline@SnO ₂ loading on flexible PET thin films for triethylamine detection at room temperature. New Journal of Chemistry, 2016, 40, 4595-4600.	2.8	17
112	NiO hierarchical hollow microspheres doped Fe to enhance triethylamine sensing properties. Materials Letters, 2018, 210, 305-308.	2.6	17
113	Facile synthesis of Pd-doped ZnSnO3 hierarchical microspheres for enhancing sensing properties of formaldehyde. Journal of Materials Science, 2019, 54, 2025-2036.	3.7	17
114	Comparison of Pd and Pd4S based catalysts for partial hydrogenation of external and internal butynes. Journal of Catalysis, 2020, 383, 51-59.	6.2	17
115	Synthesis of supported Pd nanocluster catalyst by spontaneous reduction on layered double hydroxide. Journal of Catalysis, 2020, 385, 313-323.	6.2	17
116	Synthesis of an <i>N</i> , <i>N</i> Bis(phosphonomethyl)glycine Anion-Intercalated Layered Double Hydroxide and Its Selective Infrared Absorption Effect in Low Density Polyethylene Films for Use in Agriculture. Industrial & Engineering Chemistry Research, 2010, 49, 5339-5346.	3.7	16
117	Highly efficient and selective infrared absorption material based on layered double hydroxides for use in agricultural plastic film. Applied Clay Science, 2011, 53, 592-597.	5.2	16
118	Nanoscale surface engineering of PdCo/Al2O3 catalyst via segregation for efficient purification of ethene feedstock. Chemical Engineering Science, 2019, 210, 115216.	3.8	16
119	Control of Local Electronic Structure of Pd Single Atom Catalyst by Adsorbate Induction. Small, 2022, 18, e2103852.	10.0	16
120	Intercalation of IR absorber into layered double hydroxides: Preparation, thermal stability and selective IR absorption. Materials Research Bulletin, 2012, 47, 532-536.	5.2	15
121	Controllable Synthesis and Gas-Sensing Properties of Zinc Oxide Nanocrystals With Exposed Different Percentage of Facets. IEEE Sensors Journal, 2016, 16, 866-872.	4.7	15
122	Antioxidant intercalated Zn-containing layered double hydroxides: preparation, performance and migration properties. New Journal of Chemistry, 2017, 41, 2364-2371.	2.8	15
123	Improved Electrocatalytic Performance of Tailored Metalâ€Free Nitrogenâ€Doped Ordered Mesoporous Carbons for the Oxygen Reduction Reaction. ChemElectroChem, 2018, 5, 1899-1904.	3.4	15
124	Carbon fiber paper@MgO films: in situ fabrication and high-performance removal capacity for phosphate anions. Environmental Science and Pollution Research, 2018, 25, 34788-34792.	5.3	15
125	Pd/NiO/Al Array Catalyst for 2-Ethylanthraquinone Hydrogenation: Synergistic Effect Between Pd and NiO/Al Support. Catalysis Letters, 2019, 149, 1286-1296.	2.6	15
126	Construction of a Unique Structure of Ru Sites in the RuP Structure for Propane Dehydrogenation. ACS Applied Materials & Interfaces, 2021, 13, 33045-33055.	8.0	15

#	Article	IF	CITATIONS
127	In situ topologically induced PtZn alloy @ ZnTiOx and the synergistic effect on glycerol oxidation. Applied Catalysis B: Environmental, 2021, 298, 120634.	20.2	15
128	rGO decorated ZnO/CdO heterojunction as a photoanode for photoelectrochemical water splitting. Journal of Colloid and Interface Science, 2022, 608, 2377-2386.	9.4	15
129	Improvement of Selectivity in Acetylene Hydrogenation with Comparable Activity over Ordered PdCu Catalysts Induced by Post-treatment. ACS Applied Materials & Interfaces, 2021, 13, 706-716.	8.0	15
130	A simple and promoter free way to synthesize spherical Î ³ -alumina with high hydrothermal stability. Materials Letters, 2015, 155, 75-77.	2.6	14
131	Hierarchical polyaniline microspheres loading on flexible PET films for NH ₃ sensing at room temperature. RSC Advances, 2016, 6, 6939-6945.	3.6	14
132	The role of various oxygen species in Mn-based layered double hydroxide catalysts in selective alcohol oxidation. Catalysis Science and Technology, 2017, 7, 4361-4365.	4.1	14
133	Recent Advances in Constructing Interfacial Active Catalysts Based on Layered Double Hydroxides and Their Catalytic Mechanisms. Transactions of Tianjin University, 2021, 27, 24-41.	6.4	14
134	Synthesis and Applications of Layered Double Hydroxides Based Pigments. Recent Patents on Nanotechnology, 2012, 6, 193-199.	1.3	13
135	Facile Color Tuning, Characterization, and Application of Acid Green 25 and Acid Yellow 25 Co-intercalated Layered Double Hydroxides. Industrial & Engineering Chemistry Research, 2017, 56, 5495-5504.	3.7	13
136	Pd Nanoparticles Loaded on CoAlCe Layered Double Oxide Nanosheets for Phenol Hydrogenation. ACS Applied Nano Materials, 2021, 4, 11820-11829.	5.0	13
137	Micrometer-sized dihydrogenphosphate-intercalated layered double hydroxides: synthesis, selective infrared absorption properties, and applications as agricultural films. Dalton Transactions, 2018, 47, 3144-3154.	3.3	12
138	A novel composite of α-MoO ₃ /BiVO ₄ for triethylamine selective detection. New Journal of Chemistry, 2020, 44, 2402-2407.	2.8	12
139	Design and Synthesis of Cobaltâ€Based Electrocatalysts for Oxygen Reduction Reaction. Chemical Record, 2018, 18, 840-848.	5.8	11
140	HYDROTHERMAL SYNTHESIS OF α- MoO₃ NANORODS FOR NO₂ DETECTION. International Journal of Nanoscience, 2012, 11, 1240044.	0.7	10
141	Nitrogen-Doped Ordered Mesoporous Carbons Supported Co3O4 Composite as a Bifunctional Oxygen Electrode Catalyst. Surfaces, 2019, 2, 229-240.	2.3	10
142	Preparation of AuPd/ZnO–CuO for the directional oxidation of glycerol to DHA. Catalysis Science and Technology, 2020, 10, 6223-6234.	4.1	10
143	Synergetic light stabilizing effects of reducing agent and UV absorber co-intercalated layered double hydroxides for polypropylene. Applied Clay Science, 2020, 194, 105700.	5.2	10
144	Light-Induced Structural Dynamic Evolution of Pt Single Atoms for Highly Efficient Photocatalytic CO ₂ Reduction. ACS Applied Materials & Interfaces, 2022, 14, 26752-26765.	8.0	10

#	Article	IF	CITATIONS
145	Facile synthesis of supported RuO ₂ ·xH ₂ O nanoparticles on Co–Al hydrotalcite for the catalytic oxidation of alcohol: effect of temperature pretreatment. RSC Advances, 2016, 6, 49588-49596.	3.6	9
146	Design, fabrication and anti-aging behavior of a multifunctional inorganic–organic hybrid stabilizer derived from co-intercalated layered double hydroxides for polypropylene. Inorganic Chemistry Frontiers, 2019, 6, 2539-2549.	6.0	9
147	Array Modified Molded Alumina Supported PdAg Catalyst for Selective Acetylene Hydrogenation: Intrinsic Kinetics Enhancement and Thermal Effect Optimization. Industrial & Engineering Chemistry Research, 2021, 60, 8362-8374.	3.7	9
148	Facile and surfactant-free synthesis of supported Pd nanoparticles on hydrotalcite for oxidation of benzyl alcohol. RSC Advances, 2015, 5, 74907-74915.	3.6	8
149	Fabrication of Supported Pd–Ir Mesocrystal Catalyst for Hydrogenation of 2-Ethylanthraquinone. Catalysis Letters, 2017, 147, 1802-1810.	2.6	8
150	Surfactantâ€Assisted Fabrication of Cubic Cobalt Oxide Hybrid Hollow Spheres as Catalysts for the Oxygen Reduction Reaction. ChemElectroChem, 2018, 5, 2192-2198.	3.4	8
151	HALS intercalated layered double hydroxides as an efficient light stabilizer for polypropylene. Applied Clay Science, 2019, 180, 105196.	5.2	8
152	Advances in mineral processing technologies related to iron, magnesium, and lithium. Reviews in Chemical Engineering, 2019, 36, 107-146.	4.4	8
153	An aqueous miscible organic (AMO) process for layered double hydroxides (LDHs) for the enhanced properties of polypropylene/LDH composites. New Journal of Chemistry, 2020, 44, 10119-10126.	2.8	8
154	Synthesis of hexaaluminate catalysts for methane combustion by reverse microemulsion medium. Science in China Series B: Chemistry, 2009, 52, 31-38.	0.8	7
155	Shape/Crystal Facet of Ceria Induced Well-Dispersed and Stable Au Nanoparticles for the Selective Hydrogenation of Phenylacetylene. Catalysis Letters, 2019, 149, 361-372.	2.6	7
156	Inâ€Situ Selfâ€5upporting Cobalt Embedded in Nitrogenâ€Doped Porous Carbon as Efficient Oxygen Reduction Electrocatalysts. ChemElectroChem, 2020, 7, 4024-4030.	3.4	7
157	Opening up a Radical Cross-Coupling Etherification Path by a Defect-Rich Cu/ZrO ₂ Catalyst for a High-Value Transformation of HMF. ACS Catalysis, 2022, 12, 7357-7367.	11.2	7
158	Coordinately unsaturated O _{2c} –Ti _{5c} –O _{2c} sites promote the reactivity of Pt/TiO ₂ catalysts in the solvent-free oxidation of <i>n</i> -octanol. Catalysis Science and Technology, 2021, 11, 4898-4910.	4.1	6
159	Preparation and characterization of spherical mesoporous ZrO2-Al2O3 composites with high thermal stability. Science China Chemistry, 2011, 54, 1032-1038.	8.2	5
160	Insight into the effect of support crystal form on semi-continuous oxidation of glycerol. Journal of Porous Materials, 2021, 28, 1371-1385.	2.6	5
161	Identification and Insight into the Role of Ultrathin LDHâ€Induced Dualâ€Interface Sites for Selective Cinnamaldehyde Hydrogenation. ChemCatChem, 2021, 13, 4937-4947.	3.7	5
162	Size-dependent Effect of MgAl-Layered Double Hydroxides Derived from Mg(OH)2 on Thermal Stability of Poly(vinyl chloride). Materials Today Communications, 2021, , 102851.	1.9	5

#	Article	IF	CITATIONS
163	Semi-quantitative design of synergetic surficial/interfacial sites for the semi-continuous oxidation of glycerol. Fundamental Research, 2022, 2, 412-421.	3.3	4
164	Batch and fixed-bed adsorption behavior of porous boehmite with high percentage of exposed (020) facets and surface area towards Congo red. Inorganic Chemistry Frontiers, 2021, 8, 735-745.	6.0	4
165	Rational regulation of spatially adjacent Al4c and Al6c sites assisted Ru catalysts for low-NH3 furfural tandem reductive amination. Chemical Engineering Science, 2022, 258, 117777.	3.8	4
166	Preparation and photochromic properties of NiAl-NO3-LDHs/LDPE composite. Science Bulletin, 2007, 52, 877-882.	1.7	3
167	Synthesis of Efficient Ce Modified CuO/CoAl-HT Catalysts for Styrene Epoxidation. Catalysis Letters, 2018, 148, 1589-1596.	2.6	3
168	Co-intercalated layered double hydroxides as thermal and photo-oxidation stabilizers for polypropylene. Beilstein Journal of Nanotechnology, 2018, 9, 2980-2988.	2.8	3
169	ZnO/BiFeO ₃ heterojunction interface modulation and rGO modification for detection of triethylamine. Journal of Materials Chemistry C, 2022, 10, 8015-8023.	5.5	3
170	Fabrication of Pd–Au Clusters by In Situ Spontaneous Reduction of Reductive Layered Double Hydroxides. Catalysis Letters, 2021, 151, 2355-2365.	2.6	2
171	The structural decoration of Ru catalysts by boron for enhanced propane dehydrogenation. Fundamental Research, 2022, , .	3.3	2
172	Electron-Deficient Pd clusters induced by spontaneous reduction of support defect for selective phenol hydrogenation. Chemical Engineering Science, 2022, 260, 117867.	3.8	2
173	Sensing characterization of Sn/In/Ti nanocomplex oxides for CO, CH4 and NO2. Science in China Series D: Earth Sciences, 2007, 50, 18-26.	0.9	1
174	Influence of Active Metal Precursors on the Structure and Catalytic Behavior of Pd/Al2O3 Catalysts for Selective Acetylene Hydrogenation. Catalysis Letters, 0, , 1.	2.6	1
175	Extension of inducing effect of support coordination on Ni-based ordered alloys catalyst for selective hydrogenation. Chemical Engineering Science, 2022, 260, 117852.	3.8	1